Dielectric relaxation behavior of a liquid crystal showing an unusual type of antiferroelectric-ferroelectric-antiferroelectric phase sequence

S. K. Kundu and B. K. Chaudhuri*
Solid State Physics Department, Indian Association for the Cultivation of Science, Calcutta-700032, India

A. Seed
Chemistry Department, Kent State University, Kent, Ohio 44242-0001

A. Jákli
Liquid Crystal Institute, Kent State University, Kent, Ohio 44242-0001

(Received 28 April 2002; revised manuscript received 26 December 2002; published 14 April 2003)

The temperature and frequency dependent dielectric relaxation behavior of a liquid crystalline (*S*)-(+)-1-methylheptyl 4-[2-(4-alkoxyphenyl) thiophene-5-carbonylthiooxy] benzoate system is reported. Interesting successive antiferroelectric-ferroelectric-antiferroelectric (AF-FE-AF) phase transitions are observed in this system resembling the successive phase transitions observed in crystalline Rochelle salt. The smectic-*C** (Sm*C**) to AF1 phase transition (around 103.0 °C) is first order in nature, predicted from the use of Orihara and Ishibashi theory. It is also found that a contribution of the ferroelectric Sm*C** phase ordering penetrates even in the antiferroelectric AF1 (SmC_A^*) and AF2 (SmC_A^*) phases very close to the Sm*C**-AF1 and Sm*C**-AF2 phase boundaries (critical regions). It is suggested that this type of mixing of AF and FE phases might cause surface induced ferroelectric- or ferroelectric-type ordering near the AF-FE phase transitions. A soft mode with Debye-type dispersion was observed in the Sm*A* phase. The thermal behaviors of dielectric dispersion, absorption, and dielectric strength in different phases are also reported and discussed.

DOI: 10.1103/PhysRevE.67.041704 PACS number(s): 64.70.Md, 77.84.Fa, 77.84.Nh, 61.30.−v

I. INTRODUCTION

Ferroelectric (FE) or antiferroelectric (AF) phase transitions are well known in many H-bonded molecular crystals like KH_2PO_4 [1], Rochelle salt [2], etc. However, similar ferro- and antiferroelectric ordering has also been discovered in liquid crystals (ferroelectricity in 1974 and antiferroelectricity in 1989). Since the first observation of antiferroelectricity in MHPOBC [4-(1-methylheptyloxy-carbonyl) phenyl 4′-octyloxybiphenyl 4-carboxylate] [3–5], much attention has been paid to the study of antiferroelectric liquid crystals (AFLCs) both experimentally and theoretically. Many AFLCs have also been found to show successive phase changes and other interesting behavior like frustration [6] and phase penetration [7]. An optically pure TFMHPOBC liquid crystal [8] showed a second order phase transition directly from smectic *A* (Sm*A*) to smectic C_A^* (SmC_A^*). Another antiferroelectric liquid crystal system, viz., MHPOBC, showed [4] a Sm*C** phase between Sm*A* and SmC_A^* phases. Strictly speaking, optically pure MHPOBC has three Sm*C** subphases, viz., SmC_α^*, SmC_β^*, and SmC_γ^* as reported by Fukai *et al.* [3] and Chandani *et al.* [5]. On the other hand, for mixtures of *R* and *S* enantiomers, the phase sequence changes to Sm*A*-Sm*C**-SmC_A^*, where the transition from Sm*C** to SmC_A^* is first order in nature. In recent years, a great deal of effort has also been directed to determining the detailed structures of various chiral smectic-*C* phases exhibiting antiferroelectric (SmC_A^*) or ferrielectric (SmC_{FI1}^*, SmC_{FI2}^*, SmC_α^*) electro-optic responses. Direct structural observation of superlattice periodicities associated with the AF and ferrielectric phases [9] has also been marked.

Recently an unusual antiferroelectric-ferroelectric-antiferroelectric phase sequence has been reported in an antiferroelectric (*S*)-(+)-1-methylheptyl 4-[2-(4-alkoxyphenyl) thiophene-5-carbonylthiooxy] benzoate system [10] (hereafter referred to as MHATCTB). It has the phase sequence

$$\text{cryst} \underset{67.8\,^\circ\text{C}}{\leftrightarrow} SmC_A^* \underset{103.0\,^\circ\text{C}}{\leftrightarrow} SmC^* \underset{110.0\,^\circ\text{C}}{\leftrightarrow} \text{AF2} \underset{116.0\,^\circ\text{C}}{\leftrightarrow} SmA \underset{129.0\,^\circ\text{C}}{\leftrightarrow} \text{isotropic}.$$

In this paper we report a thorough investigation of the dielectric relaxation behavior of this interesting MHATCTB system, confirming the transitions. The successive phase transitions from isotropic to crystalline phases were studied using both temperature and frequency dependent dielectric relaxation measurements. The present dielectric study supports the above phase sequence observed from differential scanning calorimetry (DSC) and polarization measurements [10]. We observed interesting phase penetration behavior,

*Author to whom correspondence should be addressed.

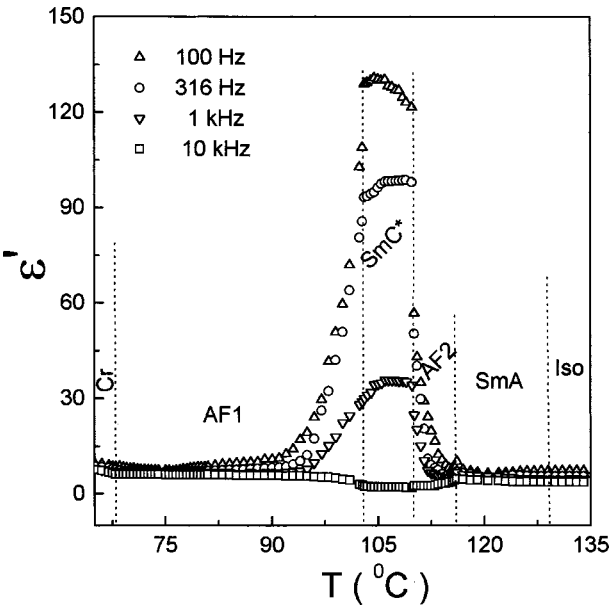

FIG. 1. Temperature dependence of the real part of the dielectric constant (ε') at different fixed frequencies for the MHATCTB system showing different phase behavior with change of temperature. The two regions of antiferroelectric phases AF1 and AF2 are also shown.

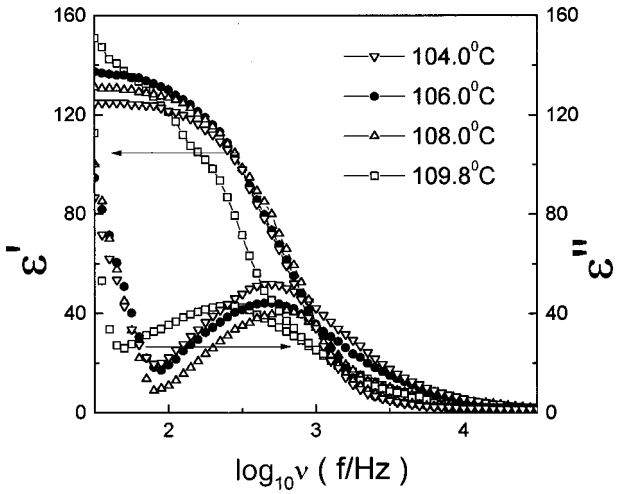

FIG. 2. Frequency dependence of the real (ε') and imaginary (ε'') parts of the dielectric constant in the ferroelectric SmC^* phase between two antiferroelectric AF1 and AF2 phases shown in Fig. 1.

which was not noted in DSC and polarization studies. We attempt to explain the nature of the AF-FE phase transition in the light of the phenomenological theory proposed by Orihara and Ishibashi [11]. The soft mode and Goldstone mode behaviors in different phases are also discussed.

II. EXPERIMENT

The method of synthesis and the phase behavior of the MHATCTB system have already been discussed by Nassif *et al.* [10]. We measured the complex dielectric permittivity in a sandwich-type cell (sample thickness $\sim 15\ \mu$m). Indium tin oxide coated glass plates were used for the electrodes. The cell was filled by the capillary action technique in the isotropic phase [12]. We used a stabilized low frequency ac (1.25 V/μm) field for better alignment of the sample, and no bias field was applied. We allowed alignment time up to 60 min. Dielectric measurements were carried out using a computer controlled Hewlett-Packard 4192A impedance analyzer having the frequency range 5 Hz–13 MHz as in [13]. The measuring temperature (60.0–135.0 °C) was controlled by using a Eurotherm temperature controller with an accuracy better than ± 0.1 °C.

III. RESULTS AND DISCUSSION

Figure 1 shows the real part of the temperature dependent dielectric constant (ε') of the antiferroelectric MHATCTB sample measured at four different fixed frequencies (viz., 100, 316, 1000, and 10 000 Hz). The observed phase sequence, viz., isotropic-SmA–AF2 (SmC_A^*)–SmC^*–AF1 (SmC_A^*)–Cr, during cooling is also presented in the same figure. The real part of the dielectric constant (ε') is found to be almost constant in the SmA phase down to 120.0 °C and then it increases gradually with decreasing temperature until the SmA-AF2 transition temperature is reached around $\sim$116.0 °C. On further cooling, the dielectric constant decreases and then increases again near the AF2-SmC^* transition point ($\sim$110.0 °C). The increase of dielectric constant near this transition temperature implies soft ferroelectric mode behavior (uniform tilt of molecules) contributing to the dielectric constant. However, the antiferroelectric mode (tilting toward opposite directions in the neighboring layers) condenses before the ferroelectric mode. In the present system, the ferroelectric SmC^* phase and the two antiferroelectric phases, viz., AF2 and AF1, are clearly separated from each other (the situation is similar to that of a crystalline Rochelle salt [2], where there are well separated para-ferro-paraelectric transitions). This type of ferro- and antiferroelectric mixing has also been observed in H-bonded ferroelectric (RbH_2PO_4) and antiferroelectric ($NH_4H_2PO_4$) mixed crystals, where local disorder and frustration leads to ''glassy'' behavior at low temperature (below 30 K) [14]. In fact, in our present system there is a mixing of the two phases near the phase boundaries (called ''critical regions''). In these critical regions both FE and AF ordering coexist. That is, there is no distinct boundary separating these two phases. To the best of our knowledge, such phase penetration behavior observed in the present antiferroelectric MHATCTB is not very common in the liquid crystal family. In the SmC^* phase, the dielectric constant is large, which implies that the Goldstone mode should exist. Since the transition from the SmC^* to the AF1 phase (around $\sim$103.0 °C) is first order in nature, predicted using Orihara and Ishibashi theory [11], the dielectric constant was expected to show a jump at the transition temperature. The experimental result, however, shows an unexpectedly small jump at the transition temperature and then gradually decreases below this transition point.

To study the dielectric relaxation processes showing up in the SmC^* phase due to the Goldstone mode, measurements of the complex dielectric permittivity ($\varepsilon^* = \varepsilon' - i\varepsilon''$) were

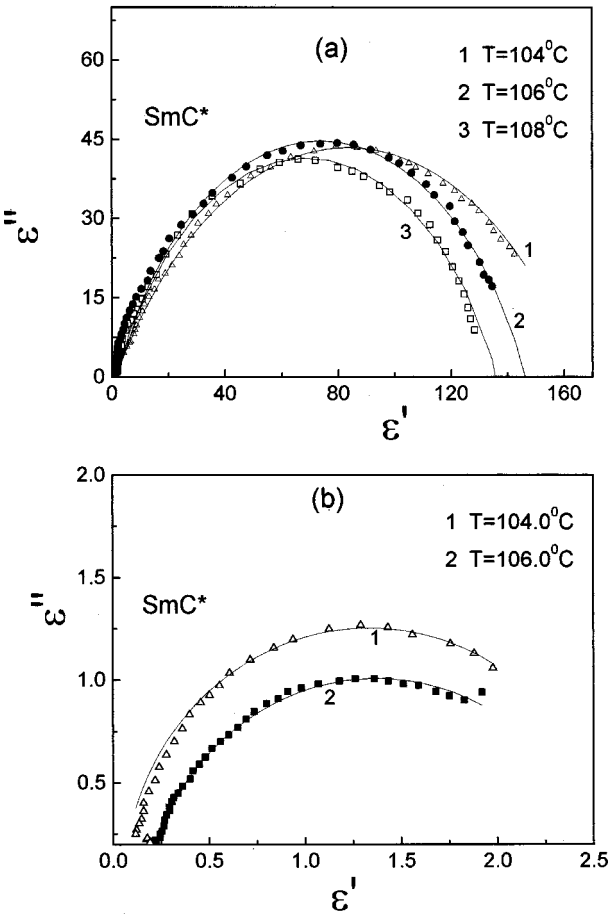

FIG. 3. Cole-Cole plots obtained for the Goldstone mode (a) and the soft mode (b) in the SmC^* phase between two antiferroelectric AF1 and AF2 phases.

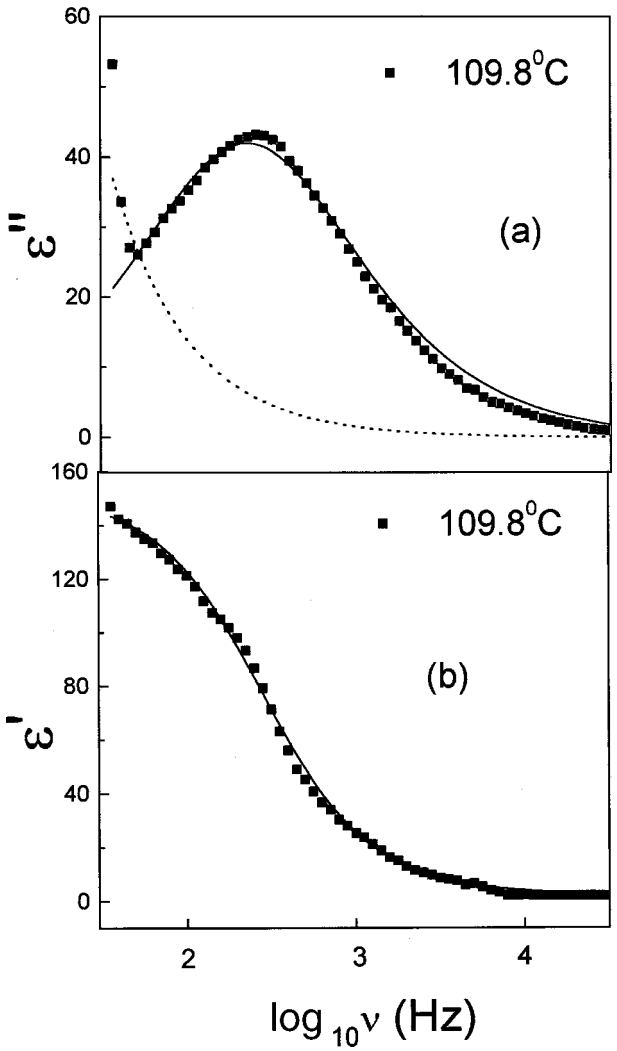

FIG. 4. Frequency dependence of (ε') and (ε'') at a fixed temperature showing conductivity contribution. Solid squares correspond to the experimental values. The dotted line shows the conductivity contribution following Eq. (3) with the fitting parameters $\delta_0 = 1.004 \times 10^{-10}\ \Omega^{-1}\,\mathrm{cm}^{-1}$ and $s = 0.04$. The solid line shows the Cole-Cole function [according to Eq. (2)].

made in the frequency range of 30 Hz–10 MHz. Figure 2 shows the real (ε') and imaginary (ε'') parts of dielectric permittivity as a function of frequency for four different fixed temperatures (viz., 104.0, 106.0, 108.0, and 109.8 °C) in the ferroelectric SmC^* phase. For the FE phase of the present MHATCTB sample, contributions to ε' and ε'' arise from the Goldstone (G) mode behavior. Figure 2 exhibits the G mode indicated by the broad peak as discussed below.

The dielectric spectra in the frequency range of 30 Hz–10 MHz, connected with the G [15] and the soft (S) [16] modes in the SmC^* phase, are shown in Fig. 3 in the forms of dispersion and absorption curves (Cole-Cole diagram). Experimental dielectric constant data (shown by the scattered points in Fig. 3) were fitted with the Cole-Cole modification of the Debye equation [17], viz.,

$$\varepsilon^* = \varepsilon_\infty + \frac{\varepsilon_s - \varepsilon_\infty}{1 + (i\omega\tau)^{1-\alpha}}, \tag{1}$$

where ε_s is the static dielectric constant, ε_∞ is the high frequency dielectric permittivity, $\tau\,[=1/(2\pi f_c)]$ and α are, respectively, the dielectric relaxation time and the distribution parameter, and f_c is the relaxation peak frequency. For a distribution of relaxation times, α varies between 0 and 1. One sees from Fig. 2 that there is a pronounced dispersion near 500 Hz connected with the G mode. The contribution of the conduction is higher at low frequencies. Its frequency dependence obeys the equation [18,19]

$$\varepsilon''(\omega) = \frac{\delta_0}{\varepsilon_0 \omega^{1-s}} \tag{2}$$

and can thereby be corrected (subtracted) as shown in Fig. 4. The fit parameters δ_0 and s are found to be consistent with other results [20]. The power law exponent (s) is generally less than 1. For the present sample s is found to be 0.04, indicating a hopping type of conductivity. It appears that the conductivity contribution appears in all the processes.

The variations of G- and S-mode critical frequencies with temperature are shown in Fig. 5. Here it would be worthwhile to mention that, although the temperature dependent dielectric constants in the antiferroelectric phase have been investigated in different types of AFLC compounds, a unique

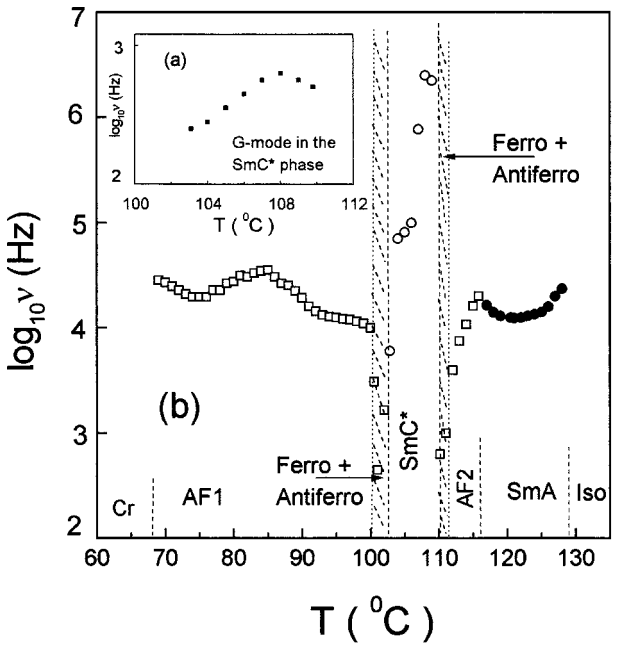

FIG. 5. (a) Variation of the *G*-mode critical frequency with temperature in the Sm*C** phase. (b) Variation of the critical frequency of different phases (AF1, Sm*C**, AF2, and Sm*A*) with temperature for MHATCTB. Here the symbol □ indicates the antiferroelectric *G* mode in the AF1 and AF2 phases, the symbol ○ indicates the *S* mode in the FE (Sm*C**) phase, and the symbol ● indicates the soft mode in the Sm*A* phase. The hatched regions indicate the phase penetration regions.

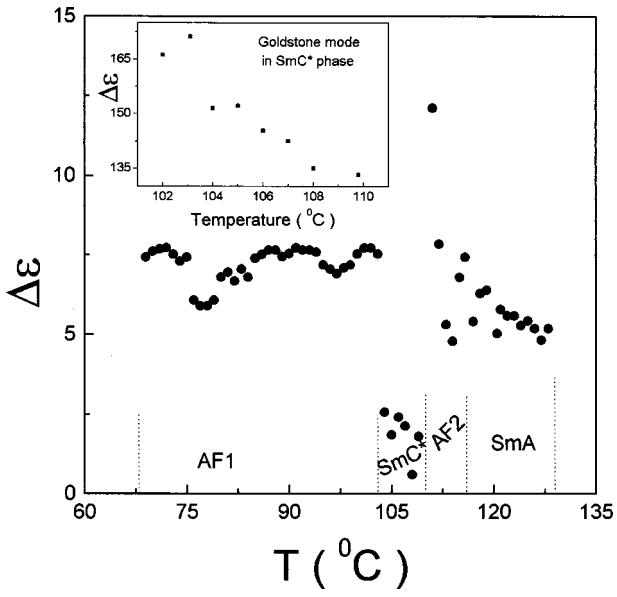

FIG. 6. Variation of the dielectric strength ($\Delta\varepsilon=\varepsilon_0-\varepsilon_\alpha$) with temperature for the Sm*A*, AF2, Sm*C**, and AF1 phases of the sample MHATCTB.

interpretation or assignment of different dielectric modes has not been possible [19,20]. The dielectric properties in AFLCs, in general, have been investigated and analyzed in the frequency range (10 Hz–13 MHz) [21–23]. In some samples, dielectric absorption studies have also been made in the ~MHz and ~kHz ranges, where the *S* mode and another different mode arise due to the director fluctuation around the molecular short axis [21]. However, there are other examples where the corresponding two modes were considered to originate, respectively, from the so-called antiphase and in-phase azimuthal angle fluctuations of the director [22]. In the present MHATCTB system, we observed the relaxation frequency at around ~10 kHz in the antiferroelectric phase in a wide range of temperature.

The relaxation of the ''ferroelectriclike Goldstone mode'' (FLGM), i.e., fluctuation of the molecules in the azimuthal plane (which is similar to the G in the ferroelectric phase) preserving the antiferroelectric ordering, was not observed in the AF1 and AF2 phases in the frequency range of our investigation. Even if such relaxation frequency does exist in the frequency ranges of our measurement, the *G* mode could not be detected. It is, however, seen from Fig. 5(b) that the *G* mode does appear at around ~2.5 °C below the AF1-Sm*C** phase transition point (~103.0 °C) and at around ~1.1 °C above the Sm*C**-AF2 phase transition (~110.0 °C). But between 100.5 and 103.0 °C and between 110.0 and 111.1 °C [the hatched regions in Fig. 5(b)], FLGMs appear in the antiferroelectric phase close to the ferroelectric-antiferroelectric phase transition region. This feature resembles the behavior observed in another antiferroelectric liquid crystal reported earlier [22,23] and also indicates some ferroelectric contribution even in the AF-FE boundary (critical) regions. This suggests that the ferroelectric phase of a particular type of ordering penetrates to a certain extent (though very small) into the antiferroelectric phase. The very small temperature regions over which such penetration occurred in the present AFLC were already mentioned above and shown in Fig. 5(b).

The variation of the distribution parameter α [shown in Eq. (1)] with temperature lies between 0.1 and 0.9. The effect of α is to produce a semicircular Cole-Cole plot, the center of which is depressed below the abscissa. The larger is α, the larger is the extent of the distribution of relaxation times. The parameter $\alpha=0$ means only one relaxation time. The variations of dielectric strength ($\Delta\varepsilon=\varepsilon_s-\varepsilon_\infty$) with temperature of the sample are shown in Fig. 6 for the AF1, Sm*C**, AF2, and Sm*A* phases.

IV. CONCLUSION

The temperature and frequency dependent dielectric constants of this antiferroelectric MHATCTB system clearly showed successive phase transitions from antiferroelectric to ferroelectric to antiferroelectric phases. It is also confirmed from the dielectric measurements of the MHATCTB liquid crystal system that a ferroelectric phase coexists between two antiferroelectric (AF1 and AF2) phases. In addition, the *G* mode observed in the Sm*C** phase is found to penetrate slightly into the antiferroelectric phase near the phase boundaries. This indicates the mixing of the ferroelectric and antiferroelectric dipolar ordering. Such mixing of ferroelectric and antiferroelectric (AF1 and AF2) phases might cause surface induced ferroelectric- or ferrielectric-type ordering near the AF-FE phase transition. This interpenetrating region will

be very important in structural and optical studies evaluating physical behavior.

ACKNOWLEDGMENTS

S.K.K. is grateful to the Council of Scientific and Industrial Research, Government of India, for financial support, and B.K.C. is grateful to Professor W. Haase and the AvH Foundation, Germany, for providing the HP frequency analyzer and the Eurotherm temperature controller used for this work. These authors also gratefully acknowledge the help offered by Somnath Roy and Suman Bandopadhyay in the computer software development.

[1] R. Blinc and B. Zeks, Adv. Phys. **21**, 693 (1972).
[2] J. Valasek, Phys. Rev. **15**, 537 (1920); **17**, 475 (1920).
[3] M. Fukui, H. Orihara, Y. Yamada, N. Yamamoto, and Y. Ishibashi, Jpn. J. Appl. Phys., Part 2 **28**, L849 (1989).
[4] A. D. L. Chandani, T. Hagiwara, Y. Suzuki, Y. Ouchi, H. Takezoe, and A. Fukuda, Jpn. J. Appl. Phys., Part 2 **27**, L729 (1988).
[5] A. D. L. Chandani, Y. Ouchi, H. Takezoe, A. Fukuda, K. Terashima, K. Furukawa, and A. Kishi, Jpn. J. Appl. Phys., Part 2 **28**, L1261 (1989).
[6] T. Matsumoto, A. Fukuda, M. Johno, Y. Motoyama, T. Yui, S-S. Seomun, and M. Yamashita, J. Mater. Chem. **9**, 2051 (1999).
[7] E. Gorecka, D. Pociecha, M. Glogarova, and J. Mieczkowski, Phys. Rev. Lett. **81**, 2946 (1998).
[8] Y. Yamada, K. Mori, N. Yamamoto, H. Hayashi, K. Nakamura, M. Yamawaki, H. Orihara, and Y. Ishibashi, Jpn. J. Appl. Phys., Part 2 **28**, L1606 (1989).
[9] P. Mach, R. Pindak, A.-M. Levelut, P. Barois, H. T. Nguyen, C. C. Huang, and L. Furenlid, Phys. Rev. Lett. **81**, 1015 (1998).
[10] L. Nassif, A. Jákli, and A. J. Seed, Mol. Cryst. Liq. Cryst. Sci. Technol., Sect. A **365**, 171 (2001).
[11] H. Orihara and Y. Ishibashi, Jpn. J. Appl. Phys., Part 2 **29**, L115 (1990).
[12] M. A. Perez Jubindo, A. Ezucer, J. Etxebarria, A. Remon, M. J. Tello, M. Marcos, and J. L. Serrano, Mol. Cryst. Liq. Cryst. **159**, 137 (1988).
[13] S. K. Kundu, E. Okabe, W. Haase, and B. K. Chaudhuri, Phys. Rev. E **64**, 051708 (2001).
[14] E. Courtens, Phys. Rev. Lett. **52**, 69 (1984).
[15] M. Pfeiffer, G. Soto, S. Wrobel, W. Haase, R. Twieg, and K. Vetterton, Ferroelectrics **121**, 55 (1991).
[16] S. Wrobel, A. M. Birader, and W. Haase, Ferroelectrics **100**, 271 (1989).
[17] K. S. Cole and R. H. Cole, J. Chem. Phys. **9**, 341 (1941).
[18] S. U. Vallerien, F. Kremer, B. Hueser, and H. W. Spieß, Colloid Polym. Sci. **267**, 583 (1989).
[19] F. N. Mott and E. A. Davis, *Electron Processes in Non-Crystalline Materials*, 2nd ed. (Clarendon, Oxford, 1979).
[20] S. K. Kundu, B. K. Chaudhuri, L. Catala, and S. Mery, Liq. Cryst. **29**, 837 (2002).
[21] H. Moritake, Y. Uchiyama, K. Myogin, M. Ozaki, and K. Yoshino, Ferroelectrics **147**, 53 (1993).
[22] M. Buivydas, F. Gouda, S. T. Lagerwall, and B. Stebler, Liq. Cryst. **18**, 879 (1995).
[23] J. W. O'Sullivan, J. K. Vij, and H. T. Nguyen, Liq. Cryst. **23**, 77 (1997).